A Second-Order Synchronous Machine Model for Multi-swing Stability Analysis

Olaoluwapo Ajala*, Alejandro Domínguez-García*, Peter Sauer*, and Daniel Liberzon†

*Department of Electrical and Computer Engineering, University of Illinois at Urbana-Champaign, Urbana, IL 61801 USA
†Coordinated Science Laboratory, University of Illinois at Urbana-Champaign, Urbana, IL 61801 USA
Email: {ooajala2, aledan, psauer, liberzon}@illinois.edu

Abstract—This paper presents a second-order model for synchronous machines that can be utilized in power system dynamic performance analysis and control design tasks. The model has a similar structure to the classical model in that it comprises two dynamic states, the power angle and the angular speed. However, unlike the classical model, the model finds applications beyond first swing stability analysis; for example, they can also be utilized in transient stability studies. The model is developed through a systematic model-order reduction of a nineteenth-order state-space model by using singular perturbation techniques. It is validated by comparing its response with that of the nineteenth-order model and that of the classical model.

I. INTRODUCTION

Dynamic models of synchronous machines find applications in power system analysis, control design tasks, and education, with each application requiring models that capture dynamical phenomena relevant to the intended use. This has led to the proliferation of synchronous machine models in the literature [1], [2], [3], [4], with varying degrees of complexity, computational cost, and state-space dimension. One such model is the so-called classical model advocated in [5] and [6], a second-order dynamic model that captures the dynamics of the machine phase and angular speed.

Analytically, the classical model is the simplest synchronous machine dynamical model, but it has certain limitations that restrict its applications to first swing stability analysis, i.e., stability analysis during the first second after a large disturbance [7], [8], [9]. As a result, if we consider that a power system may be stable in the first swing but unstable in subsequent swings, it is clear that the classical model, though simple, is unreliable beyond a one-second time interval and not suitable for certain analysis and design tasks. For example, the design of a generator synchronization scheme requires a model that captures dynamics of the generator phase, frequency and voltage magnitude over the entire synchronization period. A second-order model such as the classical model should suffice, but the first swing stability constraint makes it

inapplicable if the synchronization period exceeds one second. On the other hand, while existing high-order models, such as the two-axis model and the one-axis model [2], [10], are clearly more accurate and therefore very useful for power system simulation, they are also significantly more detailed and computationally expensive. Consequently, the high-order models are, in general, analytically intractable for such control design tasks. Therefore, there is a need to develop models that possess the simplicity of the classical model, but also the temporal breadth that it lacks.

The main contribution of this paper is the development of a second-order synchronous machine model that, when compared to the classical model, has the same state-space dimension but, unlike the classical model, can be utilized for analysis over multiple swings. Consequently, the model is significantly more accurate over a long time interval, and it is useful for a broader range of applications—an example of a usage of this model is in the development of a robust synchronization method for synchronous machines [11]. We employed singular perturbation analysis as our main tool [2], [12], [13], [14], [15] for deriving the model presented in this paper by (i) identifying the fastest dynamic states in a high-order model; (ii) developing approximate manifold equations for them, which are algebraic equations; and (iii) replacing the differential equations for these states with the algebraic counterparts.

Our approach to developing the proposed synchronous machine model is based on the developments in [2], [15], [16], where zero-order and first-order approximations of manifolds for fast dynamic states are used to develop reduced-order models. In [15], [16], the use of integral manifolds for model-order reduction is introduced with some applications presented, and in [2], the technique is used to develop the two-axis model, the one-axis model, and the classical model.

The remainder of the paper is organized as follows. In Section II, we present a synchronous machine high-order model that is adopted as the starting point for the development of our reduced order model; we also discuss the classical model. In Section III, we utilize singular perturbation analysis to develop a second-order model from the high-order model. Finally, in Section IV we validate the second-order models developed, using numerical examples. In Section V we comment on implications of the presented results.

II. PRELIMINARIES

We begin this section by presenting the high-order model of a synchronous machine adopted in this work. In addition, the time-scale properties of this model are discussed. Afterwards, we introduce the so-called classical model and describe how it can be obtained from the high-order model.

A. High-Order Synchronous Machine Model

The high-order synchronous machine model we describe in this section is a nineteenth-order state-space model that is based on developments in [2], [3]. The components included in the model are: (i) three damper windings, (ii) a wound-rotor synchronous machine, (iii) an IEEE type DC1A excitation system [17], and (iv) a Woodward diesel governor (DEGOV1) [18], coupled to a diesel engine, which acts as the prime mover. We provide mathematical expressions that describe the dynamic behavior of these components. [Note that the model is presented utilizing the $qd0$ transformation, with all parameters and variables scaled, and normalized using the per-unit system. Also, unless otherwise stated, we use 'q' and 'd' subscripts to denote quadrature axis (q-axis) and direct axis (d-axis) components of a variable or parameter, respectively].

Assumption 1. *The synchronous machine is connected to an electrical network bus through a short transmission line.*

1) Damper windings model: Let $\Phi_{q_2}(t)$ and $E_{d'}(t)$ denote the flux linkages of two damper windings aligned with the q-axis of the synchronous machine, let $\Phi_{d_1}(t)$ and $E_{q'}(t)$ denote the flux linkages of a damper winding and a field winding, respectively, aligned with the d-axis of the synchronous machine, and let I_q and I_d denote the q-axis and d-axis components of the stator output current, respectively. Then, the damper windings dynamics can be described as follows:

$$\tau_{q''}\dot{\Phi}_{q_2} = -\Phi_{q_2} - \left(X_{q'} - X_k\right)I_q - E_{d'},$$
$$\tau_{d''}\dot{\Phi}_{d_1} = -\Phi_{d_1} - \left(X_{d'} - X_k\right)I_d + E_{q'}(t), \quad (1)$$

and

$$\tau_{q'}\dot{E}_{d'} = -E_{d'} + \left(X_q - X_{q'}\right)\left(I_q - \frac{X_{q'} - X_{q''}}{(X_{q'} - X_k)^2}\left(\Phi_{q_2}\right.\right.$$
$$\left.\left. + (X_{q'} - X_k)I_q - E_{d'}\right)\right), \quad (2)$$

where X_k denotes the machine leakage reactance, X_q denotes the machine stator reactance, $X_{q'}$ and $X_{d'}$ denote machine transient reactances, $X_{q''}$ denotes the machine sub-transient reactance, and $\tau_{q''} = \frac{1}{\omega_0 R_{q_2}}\left(X_{kq_2} + X_{mq}\right)$, $\tau_{d''} = \frac{1}{\omega_0 R_{d_1}}\left(X_{k_1} + \frac{X_{md}X_{kf}}{X_{md}+X_{kf}}\right)$ and $\tau_{q'} = \frac{X_{kq_1}+X_{mq}}{\omega_0 R_{q_1}}$ are time constants, with X_{kq_2}, X_{kd_1}, X_{kf}, X_{kq_1} denoting leakage reactances, X_{mq} and X_{md} denoting mutual reactances, and R_{q_2}, R_{d_1}, R_{q_1} denoting winding resistances.

2) Stator windings and network model: Let $\Phi_q^{(s)}(t)$ and $\Phi_d^{(s)}(t)$ denote the q-axis and d-axis components of flux linkages for the stator windings, respectively, let $\Phi_q^{(e)}(t) = -X^{(e)}I_q$, and $\Phi_d^{(e)}(t) = -X^{(e)}I_d$ denote the q-axis and d-axis components of the flux linkage for the electrical line,

respectively, let $\omega^{(s)}(t)$ denote the machine angular speed in electrical radians per second, and let $\delta^{(s)}(t)$ denote the power angle of the synchronous machine in electrical radians. At the electrical network bus, let $V^{(l)}$ and $\delta^{(l)}$ denote the voltage magnitude, in per unit, and the voltage phase relative to a reference frame rotating at the nominal frequency in electrical radians, respectively. Let $V_q^{(l)} := V^{(l)}\cos\left(\delta^{(s)} - \delta^{(l)}\right)$, $V_d^{(l)} := V^{(l)}\sin\left(\delta^{(s)} - \delta^{(l)}\right)$, $\Phi_q(t) := \Phi_q^{(s)}(t) + \Phi_q^{(e)}(t)$, $\Phi_d(t) := \Phi_d^{(s)}(t) + \Phi_d^{(e)}(t)$. Then, the stator winding and network dynamics are described by:

$$\dot{\delta}^{(s)} = \omega^{(s)}(t) - \omega_0,$$
$$\frac{1}{\omega_0}\dot{\Phi}_q = -\frac{\omega^{(s)}(t)}{\omega_0}\Phi_d + V_q^{(l)} + \left(R_s + R^{(e)}\right)I_q,$$
$$\frac{1}{\omega_0}\dot{\Phi}_d = \frac{\omega^{(s)}(t)}{\omega_0}\Phi_q + V_d^{(l)} + \left(R_s + R^{(e)}\right)I_d,$$
$$\frac{1}{\omega_0}\dot{\Phi}_q^{(e)} = R^{(e)}I_q - \frac{\omega^{(s)}(t)}{\omega_0}\Phi_d^{(e)} - V_q^{(s)} + V_q^{(l)},$$
$$\frac{1}{\omega_0}\dot{\Phi}_d^{(e)} = R^{(e)}I_d + \frac{\omega^{(s)}(t)}{\omega_0}\Phi_q^{(e)} - V_d^{(s)} + V_d^{(l)},$$
$$\Phi_q = -X_{q''}^{(e)}I_q + \frac{X_{q'} - X_{q''}}{X_{q'} - X_k}\Phi_{q_2} - \frac{X_{q''} - X_k}{X_{q'} - X_k}E_{d'},$$
$$\Phi_d = -X_{d''}^{(e)}I_d + \frac{X_{d'} - X_{d''}}{X_{d'} - X_k}\Phi_{d_1} + \frac{X_{d''} - X_k}{X_{d'} - X_k}E_{q'}(t), \quad (3)$$

where $X_{q''}^{(e)} := X_{q''} + X^{(e)}$, and $X_{d''}^{(e)} := X_{d''} + X^{(e)}$, $X^{(e)}$ denotes the per-phase line reactance, $X_{d''}$ denotes a machine sub-transient reactance, $R^{(e)}$ denotes the per-phase line resistance, R_s denotes the per-phase stator resistance, and ω_0 denotes the nominal frequency in electrical radians per second.

3) Excitation system model: Let $E_f(t)$ denote the output voltage of the machines excitation system, let $U_f(t)$ denote the exciter control input, let $\bar{U}_f(t)$ denote the rate feedback variable of the voltage regulator, and let $V^{(s)} := \sqrt{\left(V_q^{(s)}\right)^2 + \left(V_d^{(s)}\right)^2}$.

Assumption 2. *The effects of magnetic saturation on the machines excitation system are negligible.*

Then, the dynamics of the machines excitation system can be described as follows:

$$\tau_{d'}\dot{E}_{q'} = -E_{q'} - (X_d - X_{d'})\left(I_d - \frac{X_{d'} - X_{d''}}{(X_{d'} - X_k)^2}\left(\Phi_{d_1}\right.\right.$$
$$\left.\left. + (X_{d'} - X_k)I_d - E_{q'}\right)\right) + E_f,$$
$$\tau_f\dot{E}_f = -K_f E_f + U_f,$$
$$\tau_u\dot{U}_f = -U_f + K_u\bar{U}_f - \frac{K_u\bar{K}_u}{\bar{\tau}_u}E_f + K_u\left(V_r^{(s)} - V^{(s)}\right),$$
$$\bar{\tau}_u\dot{\bar{U}}_f = -\bar{U}_f + \frac{\bar{K}_u}{\bar{\tau}_u}E_f, \quad (4)$$

where $V_r^{(s)}$ denotes the reference voltage magnitude, $\tau_{d'} = \frac{X_f}{\omega_0 R_f}$, $\tau_f = \frac{L_f}{K_g}$, $K_f = \frac{\bar{R}_f}{K_g}$, $\bar{\tau}_u = \frac{L_t + L_m}{R_t}$, $\bar{K}_u = \frac{N_{t2}}{N_{t2}} \frac{L_m}{R_t}$, X_d denotes the machine stator reactance, τ_u denotes the amplifier time constant, K_u denotes the amplifier gain, X_f denotes the field winding reactance, R_f denotes the field winding resistance, L_f denotes the unsaturated field inductance, K_g denotes the slope of the unsaturated portion of the exciter saturation curve, $\bar{R}_f$ denotes the exciter circuit resistance, L_t and L_m denote series and magnetizing inductances of the stabilizing transformer, which is used to stabilize the excitation system through voltage feedback [2], respectively, R_t denotes the series resistance of a stabilizing transformer, and $\frac{N_{t2}}{N_{t1}}$ denotes the turns ratio of the stabilizing transformer.

4) Prime mover and speed governor model: Let $T_m(t)$ denote the mechanical torque output of the machine. For the speed governor system, let $P_{a_2}(t)$ denote the output of its actuator, with $\dot{P}_{a_1} = P_{a_2}(t)$, and let $P_{b_2}(t)$ denote the output of its electric control box, with $\dot{P}_{b_1} = P_{b_2}(t)$. Let $\dot{P}_u = P_{a_1}(t) + \tau_4 P_{a_2}(t)$ denote the valve position of the diesel engine, which acts as the prime mover. Then, the speed control system of the synchronous machine can be expressed as follows:

$$M\dot{\omega}^{(s)} = T_m - \Phi_d(t)I_q + \Phi_q(t)I_d - \tilde{D}_0 \omega^{(s)},$$

$$\tau_m \dot{T}_m = -T_m + P_u,$$

$$\tau_{a_2} \dot{P}_{a_2} = -\frac{1}{\tau_5 + \tau_6}\left(P_{a_1}(t) - \kappa\left(P_{b_1}(t) + \tau_3 P_{b_2}\right)\right) - P_{a_2},$$

$$\tau_2 \dot{P}_{b_2} = \frac{1}{\tau_1}\left(\frac{1}{\bar{D}_0 \omega_0}(P_c - P_u) - \frac{1}{\omega_0}\left(\omega^{(s)} - \omega_0\right)\right)$$
$$- P_{b_2} - \frac{1}{\tau_1}P_{b_1}(t),$$

$$(5)$$

where τ_2, τ_3, τ_4, τ_5 and τ_6 denote time constants of the control system, $\tau_{a_2} = \frac{\tau_5 \tau_6}{\tau_5 + \tau_6}$, κ denotes a controller gain for the actuator, P_c denotes the power change setting of the machine, M denotes the inertia of the machine, $\tilde{D}_0$ denotes the friction and windage damping coefficient of the machine, τ_m denotes the time constant of the engine, and $\bar{D}_0 = \frac{1}{R_D \omega_0}$, with R_D denoting the droop coefficient. [Note that for salient pole machines, $X_q = X_{q'}$, so that $E_{d'}(t) = 0$, and for round-rotor machines, $X_q = X_d$].

B. High-Order Model Time-Scale Properties

The following observations are based on standard parameter values obtained from synchronous machine models in [1], [2], [3], [18], and an eigenvalue analysis of these models.

Observation 1. *The dynamics of* Φ_{q_2}, Φ_{d_1}, $E_{d'}$, Φ_q, Φ_d, $\Phi_q^{(e)}$, $\Phi_d^{(e)}$, $E_{q'}$, E_f, U_f, $\bar{U}_f$, T_m, P_u, P_{a_2}, P_{b_2}, P_{a_1} *and* P_{b_1}, *are much faster than those of* $\omega^{(s)}$ *and* $\delta^{(s)}$.

Observation 2. *For* $\epsilon = 0.1$, *the parameters* R_s, $\tau_{q''}$, $\tau_{q'}$, $\frac{1}{\omega_0}$, τ_f, τ_u, $\bar{\tau}_u$, τ_m, τ_{a_2}, τ_2, τ_1, $(\tau_5 + \tau_6)$, $\frac{\tau_5 \tau_6}{(\tau_5 + \tau_6)}$, $\frac{1}{\kappa R_D}$ *are* $\mathcal{O}\left(\epsilon\right)$.[1]

[1] Consider a positive constant ϵ, where $\epsilon < 1$, and a function $f(\epsilon)$, defined on some subset of the real numbers. We write $f(\epsilon) = \mathcal{O}\left(\epsilon^i\right)$ if and only if there exists a positive real number k, such that: $\left|f(\epsilon)\right| \le k\epsilon^i$, as $\epsilon \to 0$.

Based on these observations, the nineteenth-order machine model described by (1) – (5) can be expressed compactly as:

$$\dot{x}(t) = f\left(x(t), z(t), \epsilon\right), \qquad x(0) = x^0,$$
$$\epsilon \dot{z}(t) = g\left(x(t), z(t), \epsilon\right), \qquad z(0) = z^0,$$
$$(6)$$

where $x(t) = \begin{bmatrix} \delta^{(s)}, & \omega^{(s)} \end{bmatrix}^\top$, and $z(t) = \begin{bmatrix} \Phi_q, & \Phi_d, & E_{d'}, \\ \Phi_{q_2}, & \Phi_{d_1}, & \Phi_q^{(e)}, & \Phi_d^{(e)}, & E_{q'}, & E_f, & U_f, & \bar{U}_f, & T_m, \\ P_u, & P_{a_2}, & P_{b_2}, & P_{a_1}, & P_{b_1} \end{bmatrix}^\top$. In the remainder of this paper, we refer to the elements of $z(t)$ as the fast states, and the elements of $x(t)$ as the slow states. Other observations, which will prove useful in Section III, are:

Observation 3. *The dynamics of* Φ_q, Φ_d, $\Phi_q^{(e)}$ *and* $\Phi_d^{(e)}$ *are much faster than those of* Φ_{q_2}, Φ_{d_1}, $E_{d'}$ *and* $E_{q'}$.

Observation 4. *The dynamics of* Φ_{q_2} *and* Φ_{d_1} *are much faster than those of* $E_{d'}$ *and* $E_{q'}$.

C. Classical Model

The classical model of a synchronous machine is a second-order model whose formulation is based on the following assumptions [19]: (i) the machine can be modeled as a constant magnitude voltage source with a series reactance, (ii) the mechanical rotor angle of the machine can be represented by the angle of the voltage source, (iii) damping can be neglected, and (iv) the machine mechanical power input is constant. The classical model is valid only for the first swing, and according to [2], it can be derived from the high-order model by setting $\tau_{q''} = 0$, $\tau_{d''} = 0$, $\frac{1}{\omega_0} = 0$, $\frac{\omega^{(s)}(t)}{\omega_0} = 1$, $R_s = 0$, $R_e = 0$, $X_{q'} = X_{d'}$, $\tau_{q'} = \infty$, $\tau_{d'} = \infty$, $\tau_m = \infty$ to give:

$$\dot{\delta}^{(s)} = \omega^{(s)} - \omega_0,$$

$$M\dot{\omega}^{(s)} = T_m(0) - \frac{E_0}{X_{d'}^{(e)}}V^{(l)}\sin\left(\delta^{(s)} - \delta^{(l)}\right)$$
$$- \tilde{D}_0 \omega^{(s)},$$
$$(7)$$

where $E_0 = \sqrt{\left(E_{q'}(0)\right)^2 + \left(E_{d'}(0)\right)^2}$ and $X_{d'}^{(e)} := X_{d'} + X^{(e)}$ denote constants.

III. THE DAMPED MODEL: AN ACCURATE SECOND-ORDER MODEL FOR SYNCHRONOUS MACHINES

In this section, we derive a second-order model for synchronous machines that can be employed for multi-swing stability analysis, i.e., stability analysis beyond the first one second after a large disturbance. The model preserves effects of damper windings on the machines response, and we refer to it as the damped model. The following simplifying assumptions are employed in the model derivation process:

Assumption 3. *The angular speed of the machine,* $\omega^{(s)}(t)$, *is sufficiently close to the nominal speed of the machine so that* $\frac{\omega^{(s)}(t)}{\omega_0} = 1 + \mathcal{O}\left(\epsilon\right)$.

Assumption 4. *The per-phase line resistance,* $R^{(e)}$ *is* $\mathcal{O}\left(\epsilon\right)$.

The damped model is formulated by replacing the damper windings dynamical equations, (1) and (2), with algebraic

counterparts called first-order approximate manifolds, and replacing the differential equations for other fast states with algebraic counterparts called zero-order approximate manifolds. By using a first-order approximation for the damper windings manifolds, effects of damper windings on the machine response are captured by the resulting reduced model. Let $R_s^{(e)} := R_s + R^{(e)}$, $X_q^{(e)} := X_q + X^{(e)}$, $X_d^{(e)} := X_d + X^{(e)}$, $X_k^{(e)} := X_k + X^{(e)}$, $X_{q'}^{(e)} := X_{q'} + X^{(e)}$, $X_{d'}^{(e)} := X_{d'} + X^{(e)}$, $X_{q''}^{(e)} := X_{q''} + X^{(e)}$, $X_{d''}^{(e)} := X_{d''} + X^{(e)}$.

Starting with the states observed to have the fastest dynamics, $\Phi_q(t)$, $\Phi_d(t)$, $\Phi_q^{(e)}(t)$ and $\Phi_d^{(e)}(t)$, we formulate the zero-order approximate manifolds presented in the first paragraph of the Appendix. Next, for the subsequent fastest states, $\Phi_{q_2}(t)$ and $\Phi_{d_1}(t)$, which are damper winding states, we derive a first-order approximation of its manifold. Manifolds for $\Phi_{q_2}(t)$ and $\Phi_{d_1}(t)$, can be expressed as power series in $\tau_{q''}$ and $\tau_{d''}$, respectively, to give:

$$\Phi_{q_2}(t) = \Phi_{q_2,0}(t) + \tau_{q''}\Phi_{q_2,1}(t) + (\tau_{q''})^2\Phi_{q_2,2}(t) + \cdots,$$
$$\Phi_{d_1}(t) = \Phi_{d_1,0}(t) + \tau_{d''}\Phi_{d_1,1}(t) + (\tau_{d''})^2\Phi_{d_1,2}(t) + \cdots, \tag{8}$$

where '0' subscripts are used to denote a zero-order approximations, and where first-order approximations are given by:

$$\Phi_{q_2}(t) \approx \Phi_{q_2,0}(t) + \tau_{q''}\Phi_{q_2,1}(t),$$
$$\Phi_{d_1}(t) \approx \Phi_{d_1,0}(t) + \tau_{d''}\Phi_{d_1,1}(t). \tag{9}$$

Expressions for $\Phi_{q_2,0}(t)$, $\Phi_{q_2,1}(t)$, $\Phi_{d_1,0}(t)$ and $\Phi_{d_1,1}(t)$ are derived using the following steps:

- Substitute (8) into (1) to give:

$$\tau_{q''}\frac{\mathrm{d}}{\mathrm{d}t}\left(\Phi_{q_2,0}(t) + \tau_{q''}\Phi_{q_2,1}(t) + \cdots\right) = -\left(\Phi_{q_2,0}(t) + \tau_{q''}\Phi_{q_2,1}(t) + \cdots\right) - \left(X_{q'} - X_k\right)I_q - E_{d'}(t),$$
$$\tau_{d''}\frac{\mathrm{d}}{\mathrm{d}t}\left(\Phi_{d_1,0}(t) + \tau_{d''}\Phi_{d_1,1}(t) + \cdots\right) = -\left(\Phi_{d_1,0}(t) + \tau_{d''}\Phi_{d_1,1}(t) + \cdots\right) - (X_{d'} - X_k)I_d + E_{q'}(t). \tag{10}$$

- Using the zero-order approximations in (16), substitute expressions for I_q and I_d into (10) and equate the $(\tau_{q''})^0$, $(\tau_{d''})^0$, $(\tau_{q''})^1$ and $(\tau_{d''})^1$ terms to give:

$$\Phi_{q_2,0}(t) = -\frac{X_k^{(e)}}{X_{q'}^{(e)}}E_{d'}(t) - \frac{X_{q'} - X_k}{X_{q'}^{(e)}}V^{(l)}\sin(\delta^{(s)}(t) - \delta^{(l)}),$$

$$\Phi_{d_1,0}(t) = \frac{X_k^{(e)}}{X_{d'}^{(e)}}E_{q'}(t) + \frac{X_{d'} - X_k}{X_{d'}^{(e)}}V^{(l)}\cos(\delta^{(s)}(t) - \delta^{(l)}),$$

$$\Phi_{q_2,1}(t) = -\frac{X_{q''}^{(e)}X_k^{(e)}}{\tau_{q'}(X_{q'}^{(e)})^3}(X_q^{(e)}E_{d'}(t) - (X_q - X_{q'})V^{(l)}$$
$$\cdot\sin(\delta^{(s)}(t) - \delta^{(l)})) + \frac{X_{q''}^{(e)}(X_{q'} - X_k)}{(X_{q'}^{(e)})^2}\dot{V}_d^{(l)},$$

$$\Phi_{d_1,1}(t) = \frac{X_{d''}^{(e)}X_k^{(e)}}{\tau_{d'}(X_{d'}^{(e)})^3}(X_d^{(e)}E_{q'}(t) - (X_d - X_{d'})V^{(l)}$$
$$\cdot\cos(\delta^{(s)}(t) - \delta^{(l)})) - \frac{X_{d''}^{(e)}(X_{d'} - X_k)}{(X_{d'}^{(e)})^2}\dot{V}_q^{(l)}$$
$$- \frac{X_{d''}^{(e)}X_k^{(e)}}{\tau_{d'}(X_{d'}^{(e)})^2}E_f(t),$$

where $\dot{V}_d^{(l)} = V^{(l)}\cos(\delta^{(s)}(t) - \delta^{(l)})(\dot{\delta}^{(s)}(t) - \dot{\delta}^{(l)}) + \dot{V}^{(l)}\sin(\delta^{(s)}(t) - \delta^{(l)})$, $\dot{V}_q^{(l)} = \dot{V}^{(l)}\cos(\delta^{(s)}(t) - \delta^{(l)}) - V^{(l)}\sin(\delta^{(s)}(t) - \delta^{(l)})(\dot{\delta}^{(s)}(t) - \dot{\delta}^{(l)})$. Next, for the damper winding state observed to have the slower dynamics, $E_{d'}(t)$, we derive a first-order approximation of its manifold. A manifold for $E_{d'}(t)$ can be expressed as a power series in $\tau_{q'}$ to give:

$$E_{d'}(t) = E_{d',0}(t) + \tau_{q'}E_{d',1}(t) + (\tau_{q'})^2E_{d',2}(t) + \cdots, \tag{11}$$

from where it follows that a first-order approximation is given by:

$$E_{d'}(t) \approx E_{d',0}(t) + \tau_{q'}E_{d',1}(t). \tag{12}$$

Expressions for $E_{d',0}(t)$ and $E_{d',1}(t)$ can be derived using the following steps:

- Substitute (9) and (11) into (2) to give:

$$\tau_{q'}\frac{\mathrm{d}}{\mathrm{d}t}(E_{d',0}(t) + \tau_{q'}E_{d',1}(t) + \cdots) =$$
$$- (E_{d',0}(t) + \tau_{q'}E_{d',1}(t) + \cdots)$$
$$+ (X_q - X_{q'})\left(I_q - \frac{X_{q'}(X_{q'} - X_{q''})}{X_{q''}(X_{q'} - X_k)^2}\tau_{q''}\Phi_{q_2,1}(t)\right). \tag{13}$$

- Using the zero-order approximations in (16), substitute the expressions for I_q and $\Phi_{q_2,1}(t)$, into (13), and equate the $(\tau_{q'})^0$ and $(\tau_{q'})^1$ terms to give:

$$E_{d',0}(t) = \frac{X_q - X_{q'}}{X_q^{(e)}}V^{(l)}\sin(\delta^{(s)}(t) - \delta^{(l)}) - \frac{N_q}{D_q}\dot{V}_d^{(l)},$$

$$E_{d',1}(t) = -\frac{N_{q'}}{\tilde{D}_q}\dot{V}_d^{(l)} + \mathcal{O}(\tau_{q'}),$$

where $N_q = \tau_{q'}\tau_{q''}X_{q'}^{(e)}X_k^{(e)}(X_q - X_{q'})(X_{q'} - X_{q''})(X_{q'} - X_k)$, $D_q = \tau_{q'}X_q^{(e)}(X_{q'}^{(e)})^2(X_{q'} - X_k)^2 - \tau_{q''}X_q^{(e)}(X_k^{(e)})^2(X_q - X_{q'})(X_{q'} - X_{q''})$, $N_{q'} = \tau_{q'}(X_{q'}^{(e)})^3(X_q - X_{q'})(X_{q'} - X_k)^2$, and $\tilde{D}_q = X_q^{(e)}D_q$. Finally, for other states observed to have fast dynamics, i.e., $E_{q'}$, E_f, U_f, $\bar{U}_f$, T_m, P_u, P_{a_2}, P_{b_2}, P_{a_1}, and P_{b_1}, zero-order manifolds are derived as described in the Appendix.

Substituting the first-order approximate manifolds in (9) and (12), and the zero-order approximate manifolds in (16) and (17), into (1)–(5), and setting $\mathcal{O}\left((\tau_{q'})^2\right)$ terms to zero, the damped model for synchronous machines is given by:

$$\dot{\delta}^{(s)} = \omega^{(s)} - \omega_0,$$

$$M\dot{\omega}^{(s)} = P_r^{(s)} - D_0\omega^{(s)} - \frac{C_x}{2}\left(V^{(l)}\right)^2\sin 2\left(\delta^{(s)} - \delta^{(l)}\right)$$
$$- \frac{C_k}{X_d^{(e)}}\left(V_r^{(s)} - V^{(s)}\right)V^{(l)}\sin\left(\delta^{(s)} - \delta^{(l)}\right)$$
$$- C_q\left(V^{(l)}\right)^2\cos^2\left(\delta^{(s)} - \delta^{(l)}\right)\left(\dot{\delta}^{(s)} - \dot{\delta}^{(l)}\right)$$
$$- C_d\left(V^{(l)}\right)^2\sin^2\left(\delta^{(s)} - \delta^{(l)}\right)\left(\dot{\delta}^{(s)} - \dot{\delta}^{(l)}\right)$$
$$- \frac{(C_q - C_d)}{2}\dot{V}^{(l)}V^{(l)}\sin 2\left(\delta^{(s)} - \delta^{(l)}\right), \tag{14}$$

where $P_r^{(s)} = P_c + \bar{D}_0\omega_0$, $D_0 = \bar{D}_0 + \tilde{D}_0$, C_k, C_x, C_q, and C_d are constants,

$C_k = \frac{K_u}{K_f}$, $C_x = \frac{(X_d - X_q)}{X_q^{(e)} X_d^{(e)}}$, $C_q = C_{q''} + \left(C_{q'} + \tilde{C}_{q''}\right)^2 \tilde{C}_q$,

with $C_{q''} = \frac{\tau_{q''}(X_{q'} - X_{q''})}{\left(X_{q'}^{(e)}\right)^2}$, $\tilde{C}_q = \frac{(X_q - X_{q'})}{\bar{D}_q}$, $C_{q'} =$

$\tau_{q'} X_{q'}^{(e)} \left(X_{q'} - X_k\right)$, $\tilde{C}_{q''} = \frac{\tau_{q''} X_q^{(e)} X_k^{(e)} \left(X_{q'} - X_{q''}\right)}{X_{q'}^{(e)}}$,

and $C_d = C_{d''} + \left(C_{d'} + \tilde{C}_{d''}\right) \tilde{C}_{d''} \tilde{C}_d$, with

$C_{d''} = \frac{\tau_{d''}(X_{d'} - X_{d''})}{\left(X_{d'}^{(e)}\right)^2}$, $\tilde{C}_d = \frac{(X_d - X_{d'})}{\tilde{D}_d}$, $C_{d'} =$

$\tau_{d'} X_{d'}^{(e)} \left(X_{d'} - X_k\right)$, $\tilde{C}_{d''} = \frac{\tau_{d''} X_d^{(e)} X_k^{(e)} \left(X_{d'} - X_{d''}\right)}{X_{d'}^{(e)}}$.

C_q, C_d, C_k are positive constants, whereas C_x is a nonnegative constant. For salient pole machines, $\tilde{C}_q = 0$, whereas for round-rotor machines, $C_x = 0$.

Assumption 5. *The voltage support of the synchronous machine is such that: (i) the voltage magnitude at the electrical network bus, i.e., $V^{(l)}$, is approximately constant at 1 per-unit, and (ii) the steady state voltage error of the synchronous machine, i.e., $V_r^{(s)} - V^{(s)}$, is approximately constant.*

Using Assumption 5, a simplified form of the damped model, which was employed in [11], is formulated as follows. Let $V_r^{(s)} - V^{(s)} = 1$ and $V^{(l)} = 1$. It follows that, for $\theta^{(s)} := \delta^{(s)} + \omega_0 t$, and $\theta^{(l)} := \delta^{(l)} + \omega_0 t$, the damped model is described by:

$$\dot{\theta}^{(s)} = \omega^{(s)},$$
$$M\dot{\omega}^{(s)} = P_r^{(s)} - P^{(l)}(t) - D_0 \omega^{(s)}, \qquad (15)$$

where $P_r^{(s)} = P_c + \bar{D}_0 \omega_0$, $D_0 = \bar{D}_0 + \tilde{D}_0$, $P^{(l)}(t) = K_1 \sin(\theta^{(s)} - \theta^{(l)}) + X_1 \sin 2(\theta^{(s)} - \theta^{(l)}) + (C_1 \cos^2(\theta^{(s)} - \theta^{(l)}) + C_2 \sin^2(\theta^{(s)} - \theta^{(l)}))(\dot{\theta}^{(s)} - \dot{\theta}^{(l)})$. With $C_1 = C_q$, $C_2 = C_d$, $K_1 = \frac{C_k}{X_d^{(e)}}$, and $X_1 = \frac{C_x}{2}$, C_1, C_2, K_1 are positive constants, whereas X_1 is a nonnegative constant.

IV. NUMERICAL VALIDATION

In this section, simulation results comparing the high-order model, the classical model, and the damped model of a round-rotor synchronous machine are presented. We consider a two-bus power system with a synchronous machine connected to a constant power load through a short electrical transmission line. See Fig. 1 for a one-line diagram, and Table I for the system parameters. In this test case, we consider the system
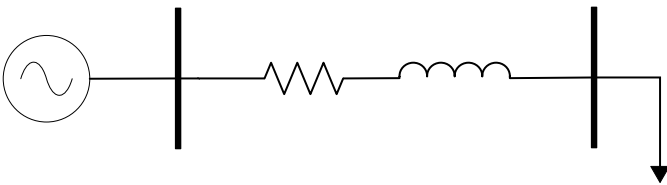

Fig. 1: One line diagram of a power system with a synchronous machine connected to a constant power load through a short transmission line.

response to an increase in active power demanded by the load. A stable equilibrium point of the high-order model is

chosen as the common initial condition for all the models. The loads active power demand is increased from 0.05 [pu] to 0.25 [pu] at time $t = 30$ [s], and the reference voltage magnitude $V_r^{(s)}$ is changed at time $t = 30$ [s] to keep the bus voltage magnitude at $V^{(l)} = 1$ [pu]. The numerical results presented in Fig. 2 show that the damped model has an overall better accuracy than the classical model, and that after the first one second following the disturbance, the inaccuracy of the classical model increases exponentially.

TABLE I: System parameters for a salient pole synchronous machine

	parameter	value
Damper windings	$\tau_{q''}$	0.9453 [s]
	$\tau_{d''}$	0.042 [s]
	$\tau_{q'}$	3.6123 [s]
	$X_{q''}$	0.2388 [pu]
	$X_{q'}$	0.7299 [pu]
	X_q	1.7997 [pu]
	X_k	0.19 [pu]
Stator windings	ω_0	376.99 [rad/s]
	R_s	0.003 [pu]
	$X_{d''}$	0.24 [pu]
	$X_{d'}$	0.32 [pu]
IEEE DC1A exciter	$\tau_{d'}$	5.0141 [s]
	τ_f	1×10^{-8} [s]
	τ_u	0.002 [s]
	$\bar{\tau}_u$	1×10^{-12} [s]
	X_d	1.7997 [pu]
	K_f	1 [pu]
	K_u	200
	$\bar{K}_u$	0 [s]
DEGOV1 speed governor	τ_1	1×10^{-4} [s]
	τ_2	0 [s]
	τ_3	0.5001 [s]
	τ_4	25×10^{-3} [s]
	τ_5	9×10^{-4} [s]
	τ_6	5.74×10^{-3} [s]
	τ_m	24×10^{-3} [s]
	κ	10
	$P_r^{(s)}$	0 [pu]
	M	0.1188 [s²]
	$\tilde{D}_0$	2.5825×10^{-7} [s/rad]
	$\bar{D}_0$	0.0531 [s/rad]
Transmission line	$R^{(e)}$	0.004 [pu]
	$X^{(e)}$	0.0595 [pu]

V. CONCLUDING REMARKS

In this paper, we introduced the damped model for synchronous machines. We also showed how this model and the so-called classical model can be derived from a high-order machine model. While the classical model is derived by identifying small and large parameters in the high-order model, and setting them to zero and infinity, respectively, the damped model is derived by identifying fast and slow states in the high-order model, and replacing differential equations for the fast states with algebraic counterparts, referred to as approximate manifolds (zero-order or first-order). The damped model was validated by comparing its response to those of a high-order model and the classical model, for given test cases.
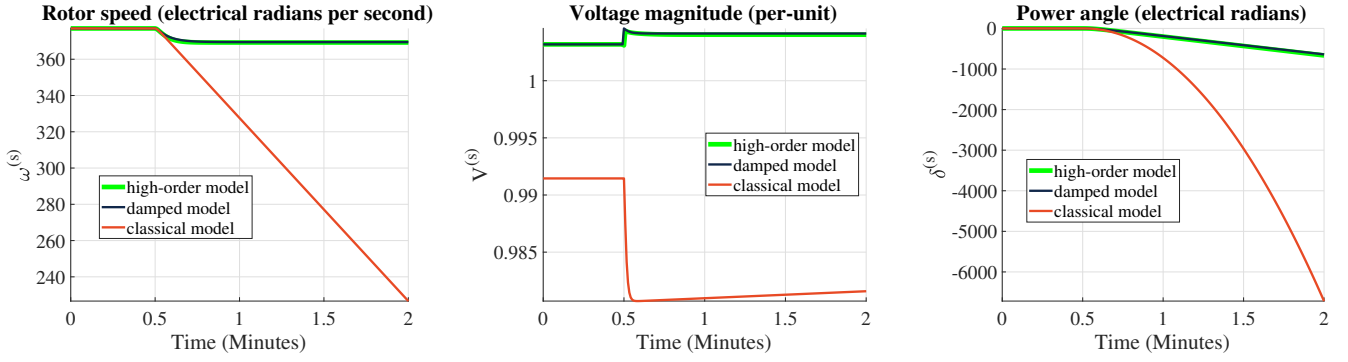
Fig. 2: Machine angular speed, voltage magnitude, and phase.

APPENDIX

In this section, we present the zero-order approximate manifolds for the fast states identified in Section II-B. These manifolds are used in our formulation of the damped model. The following zero-order manifolds were developed by setting $R_s = 0$, $R^{(e)} = 0$, $\frac{1}{\omega_0} = 0$ and $\frac{\omega^{(s)}(t)}{\omega_0} = 1$:

$$
\begin{aligned}
\Phi_{q,0}(t) &= -V^{(l)} \sin\left(\delta^{(s)}(t) - \delta^{(l)}\right), \\
\Phi_{d,0}(t) &= V^{(l)} \cos\left(\delta^{(s)}(t) - \delta^{(l)}\right), \\
\Phi_{q,0}^{(e)}(t) &= V_d^{(s)} - V^{(l)} \sin\left(\delta^{(s)}(t) - \delta^{(l)}\right), \\
\Phi_{d,0}^{(e)}(t) &= -V_q^{(s)} + V^{(l)} \cos\left(\delta^{(s)}(t) - \delta^{(l)}\right),
\end{aligned}
\tag{16}
$$

where '0' subscripts are used to denote a zero-order approximations, and from where it follows that:
$I_q = \frac{(X_{q'} - X_{q''})}{(X_{q'} - X_k)(X_{q''}^{(e)})} \Phi_{q_2}(t) - \frac{(X_{q''} - X_k)}{(X_{q'} - X_k)(X_{q''}^{(e)})} E_{d'}(t) + \frac{V^{(l)} \sin\left(\delta^{(s)}(t) - \delta^{(l)}\right)}{X_{q''}^{(e)}}$, and $I_d = \frac{(X_{d'} - X_{d''})}{(X_{d'} - X_k)(X_{d''}^{(e)})} \Phi_{d_1}(t) + \frac{(X_{d''} - X_k)}{(X_{d'} - X_k)(X_{d''}^{(e)})} E_{q'}(t) - \frac{V^{(l)} \cos\left(\delta^{(s)}(t) - \delta^{(l)}\right)}{X_{d''}^{(e)}}$. The following zero-order manifolds were developed by setting $\tau_{d'}$, and all $\mathcal{O}(\epsilon)$ parameters except $\tau_{q''}$ and $\tau_{q'}$, to zero to give:

$$
\begin{aligned}
E_{f,0}(t) &= \frac{K_u(V_r^{(s)} - V^{(s)})}{K_f}, \qquad T_{m,0}(t) = P_{u,0}(t), \\
P_{u,0}(t) &= P_c - \bar{D}_0(\omega^{(s)}(t) - \omega_0), \qquad P_{b_1,0}(t) = 0, \\
P_{b_2,0}(t) &= 0, \qquad P_{a_1,0}(t) = 0, \qquad P_{a_2,0}(t) = 0, \\
U_{f,0}(t) &= K_f E_{f,0}(t), \qquad \bar{U}_{f,0}(t) = \frac{\bar{K}_u}{\bar{\tau}_u} E_{f,0}(t), \\
E_{q',0}(t) &= \frac{X_{d'}^{(e)}}{X_d^{(e)}} E_{f,0}(t) - \frac{N_d}{D_d} \dot{V}_q^{(l)} \\
&\quad + \frac{X_d - X_{d'}}{X_d^{(e)}} V^{(l)} \cos(\delta^{(s)}(t) - \delta^{(l)}),
\end{aligned}
\tag{17}
$$

where $N_d = \tau_{d'} \tau_{d''} X_{d'}^{(e)} X_k^{(e)} (X_d - X_{d'})(X_{d'} - X_{d''})(X_{d'} - X_k)$, and $D_d = \tau_{d'} X_d^{(e)} (X_{d'}^{(e)})^2 (X_{d'} - X_k)^2 - \tau_{d''} X_d^{(e)} (X_k^{(e)})^2 (X_d - X_{d'})(X_{d'} - X_{d''})$.

REFERENCES

[1] P. Kundur, N. J. Balu, and M. G. Lauby, *Power system stability and control*. McGraw-Hill, 1994.

[2] P. Sauer and A. Pai, *Power System Dynamics and Stability*. Stipes Publishing L.L.C., 2006.

[3] P. Krause, O. Wasynczuk, S. Sudhoff, and S. Pekarek, *Analysis of Electric Machinery and Drive Systems*, ser. IEEE Press Series on Power Engineering. Wiley, 2013.

[4] L. Wang, J. Jatskevich, and H. W. Dommel, "Re-examination of synchronous machine modeling techniques for electromagnetic transient simulations," *IEEE Transactions on Power Systems*, vol. 22, no. 3, pp. 1221–1230, Aug. 2007.

[5] S. Crary, *Power System Stability: Transient stability*, ser. General Electric series. John Wiley, 1947.

[6] E. Kimbark, *Power Systems Stability. Vol. 3. Synchronous Machines*. Wiley, 1956.

[7] A. Pai, *Energy Function Analysis for Power System Stability*, ser. Power Electronics and Power Systems. Springer, Boston, MA, 1989.

[8] P. M. Anderson and A. A. Fouad, *Power system control and stability*, ser. IEEE Press power engineering series. IEEE Press, 2003.

[9] S. Y. Caliskan and P. Tabuada, "Uses and abuses of the swing equation model," in *Proc. of IEEE Conference on Decision and Control (CDC)*, Dec. 2015, pp. 6662–6667.

[10] T. Weckesser, H. Jóhannsson, and J. Østergaard, "Impact of model detail of synchronous machines on real-time transient stability assessment," in *Proc. of the IREP Symposium Bulk Power System Dynamics and Control - IX Optimization, Security and Control of the Emerging Power Grid*, Aug. 2013, pp. 1–9.

[11] O. Ajala, A. D. Domínguez-García, and D. Liberzon, "An approach to robust synchronization of electric power generators," in *Proc. of the IEEE Conference on Decision and Control (CDC)*, Dec. 2018, pp. 1586–1591.

[12] P. Kokotović, H. K. Khalil, and J. O'Reilly, *Singular Perturbation Methods in Control: Analysis and Design*, ser. Classics in Applied Mathematics. Society for Industrial and Applied Mathematics, 1986.

[13] H. K. Khalil, *Nonlinear Systems*. Pearson Education, Limited, 2013.

[14] J. H. Chow, *Time-Scale Modeling of Dynamic Networks with Applications to Power Systems*, B. A.V. and T. M., Eds. Springer, 1982.

[15] P. W. Sauer, S. Ahmed-Zaid, and P. V. Kokotovic, "An integral manifold approach to reduced order dynamic modeling of synchronous machines," *IEEE Transactions on Power Systems*, vol. 3, no. 1, pp. 17–23, Feb. 1988.

[16] P. V. Kokotovic and P. W. Sauer, "Integral manifold as a tool for reduced-order modeling of nonlinear systems: A synchronous machine case study," *IEEE Transactions on Circuits and Systems*, vol. 36, no. 3, pp. 403–410, Mar. 1989.

[17] "IEEE Recommended Practice for Excitation System Models for Power System Stability Studies," *IEEE Std 421.5-2016 (Revision of IEEE Std 421.5-2005)*, pp. 1–207, Aug. 2016.

[18] PowerWorld corporation. (2017) Woodward diesel governor model. [Online]. Available: {https://www.powerworld.com}

[19] A. Fouad and V. Vittal, *Power System Transient Stability Analysis Using the Transient Energy Function Method*. Prentice Hall, 1992.